THE OHIO STATE UNIVERSITY

Constitutive Parameter Extraction for Heated Materials

J. Munk and A. Dominek

The Ohio State University

ElectroScience Laboratory

Department of Electrical Engineering
Columbus, Ohio 43212

Annual Report 723224-2
Grant No. NAG3-1108
February 1991

National Aeronautics and Space Administration
Lewis Research Center
21000 Brookpark Rd.
Cleveland, OH 44135

50272-101

REPORT DOCUMENTATION PAGE	1. REPORT NO.	2.	3. Recipient's Accession No.

4. Title and Subtitle

Constitutive Parameter Extraction for Heated Materials

5. Report Date
February 1991

6.

7. Author(s)
J. Munk and A. Dominek

8. Performing Org. Rept. No.
723224-2

9. Performing Organization Name and Address
The Ohio State University
ElectroScience Laboratory
1320 Kinnear Road
Columbus, OH 43212

10. Project/Task/Work Unit No.

11. Contract(C) or Grant(G) No.
(C)
(G) NAG3-1108

12. Sponsoring Organization Name and Address
National Aeronautics and Space Administration
Lewis Research Center
21000 Brookpark Rd., Cleveland, OH 44135

13. Report Type/Period Covered
Annual Report

14.

15. Supplementary Notes

16. Abstract (Limit: 200 words)

The focus of this report is the determination of the electrical constitutive parameters of material with general complex ϵ and μ values at elevated temperatures. Measurement fixtures and techniques are evaluated for frequencies between 8 and 12 GHz using a rectangular waveguide with the sample completely filling the fixture. Three different measurement techniques are evaluated to obtain the necessary measured quantities for parameter extraction. The most desirable technique used two reflection measurements from material samples of different thicknesses backed with a short. Temperatures up to 600° F were investigated.

17. Document Analysis a. Descriptors

ABSORBERS
DIELECTRIC
MATERIALS
MEASUREMENT

b. Identifiers/Open-Ended Terms

c. COSATI Field/Group

18. Availability Statement	19. Security Class (This Report)	21. No. of Pages
A. Approved for public release; Distribution is unlimited.	Unclassified	46
	20. Security Class (This Page) Unclassified	22. Price

(See ANSI-Z39.18) *See Instructions on Reverse* OPTIONAL FORM 272 (4-77)
Department of Commerce

Contents

List of Figures

Chapter 1

Introduction

The main focus of this report is the extraction of the electromagnetic constitutive parameters at elevated temperatures. The parameters of interest are the complex permittivity and permeability values denoted with reference symbols of ϵ and μ, respectively [1]. Of the two basic techniques commonly used [2], i.e., the resonance and transmission line, the transmission line is considered here due to its broadband capability and greater tolerance to changes in measured values from fixture variations associated with temperature dependencies.

The ability to relate constitutive parameters from measured reflection and transmission characteristics is readily done when the cross section of a transmission line is completely filled. Performing these measurements when changes in fixture dimensions or a gap results between the fixture and material sample due to temperature dependencies can result in errors. Errors due to fixture variation can be controlled through proper fixture design and calibration procedures. Accounting for error gaps between the sample and fixture is not as direct [3].

The presented material focuses upon several aspects for elevated temperature measurements. The upper temperature used for these measurements

was 500° F but the concepts can be extended for higher temperature measurements. The first consideration pertains to fixture designs based on the sources of errors. These errors are a result of temperature expansion of the fixture. Some of these errors may be minimized through a proper calibration technique. The next consideration is determining the most appropriate de-embedding technique. Three different approaches will be examined. Finally, the performance of the most stable approach will be experimentally examined.

Chapter 2

Fixture Considerations

The two most common transmission line fixtures are coaxial and rectangular waveguide fixtures. Both fixtures are operated in the frequency band of dominant mode excitation. The coaxial fixture has the best bandwidth since its dominant mode has no cutoff frequency. The smallest frequency a rectangular guide can operate at where is the wavelength is twice the dimension of the width of the guide.

Sample preparation is the simplest in the rectangular guide since just a rectangular sample is required. Greater care is required for the coaxial fixture samples since concentric perimeters are needed. It is important for both fixtures to have tight fitting samples since the most desirable de-embedded technique requires a completely filled cross section. Allowing air gaps which may occur due to thermal expansion will result in errors, especially when the electric field is polarized normal to the gap's surfaces. The coaxial fixture is most susceptible since the electric field of the dominant mode is always normal to any gap. The rectangular guide only experiences this sensitivity when the gap occurs along the longest side walls. Figure 2.1 illustrates the electric field distribution for the dominant mode for each fixture.

Another source of error can occur when the fixture dimensions change

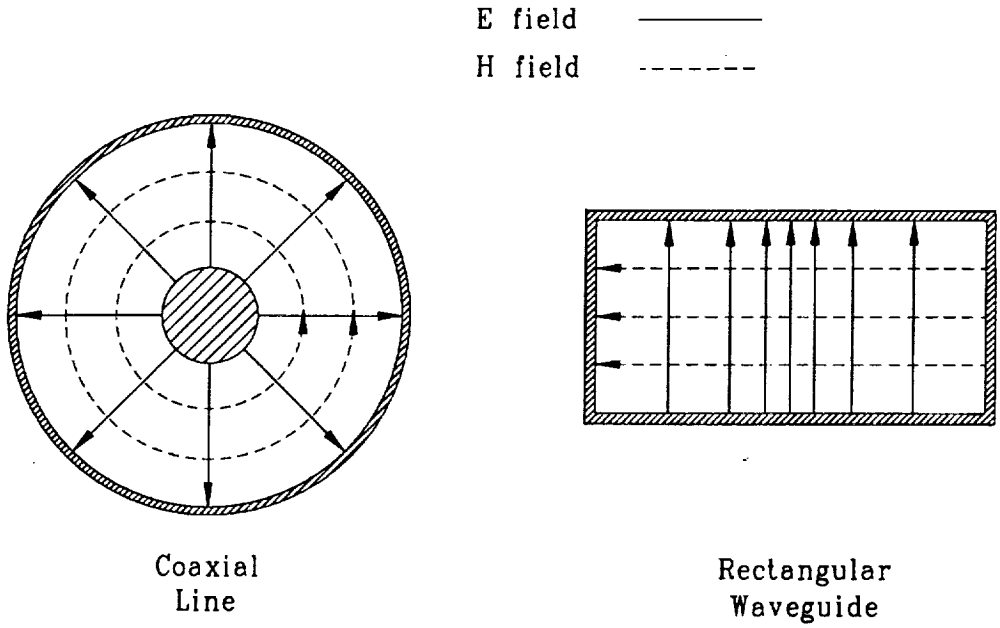

Figure 2.1: Electric field illustration for the dominant mode in coaxial and rectangular fixtures.

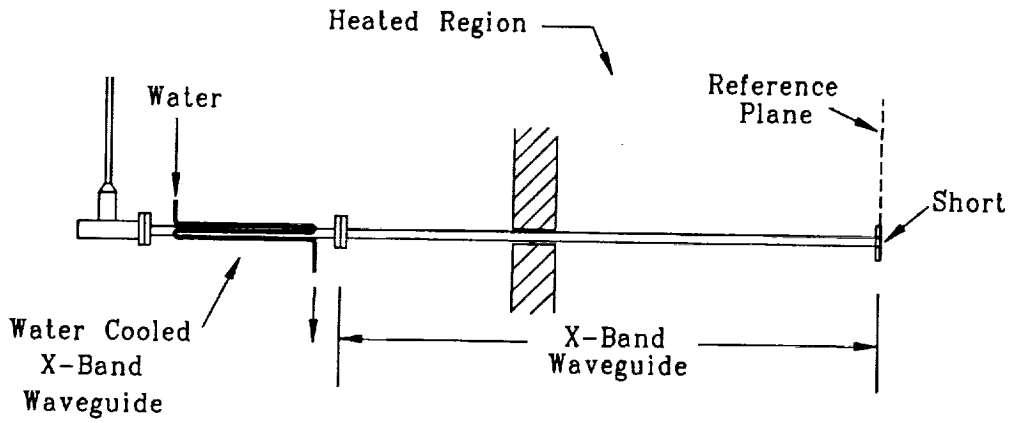

Figure 2.2: Heated waveguide setup.

as a function of temperature. One source of error arises in the change of the relative location of the calibration reference plane due to an elongation of the fixture's length. However, this is not the only change that will occur. Deformation of the fixture's cross section will also occur and perturb the measurements. These perturbations can require that a calibration be performed at the operational temperature.

The effects of heating the waveguide were measured by inserting the shorted end of the fixture in an electric oven and observing the reflected field as a function of temperature. The calibrated results are shown in Figures 2.3 through 2.5. The calibration technique used is discussed in [5, 6] and was performed at room temperature. Figure 2.2 illustrates the experimental setup used to heat the dielectric samples.

Figures 2.3 through 2.5 indicate that, although there is a change in phase as a function of temperature, this change seems to be relatively constant as a function of frequency. It was initially felt that the increased length of the waveguide would cause the phase of the heated short to change as a function of frequency. However, it is necessary to consider that the width of the

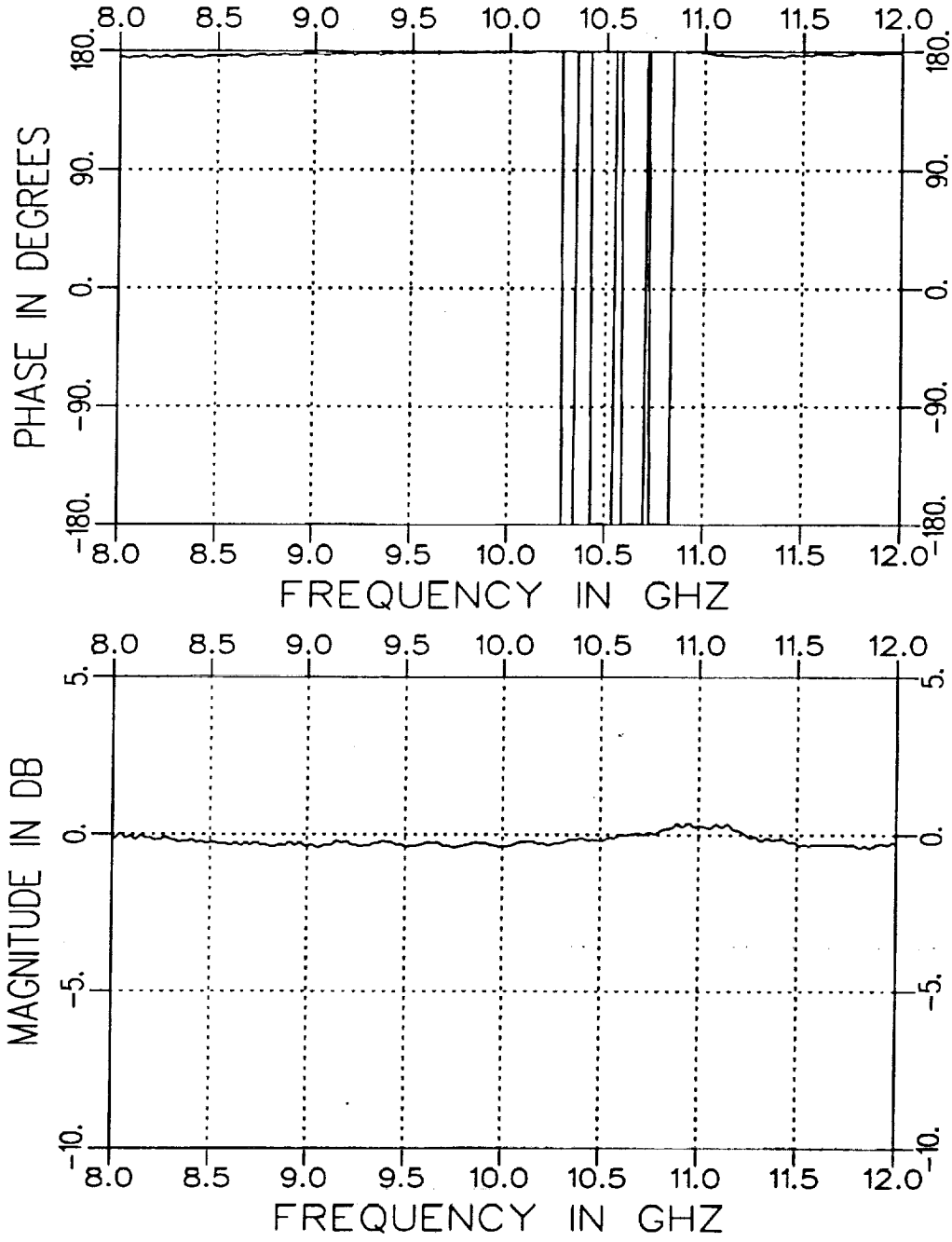

Figure 2.3: Measured reflection from a short at 300° F.

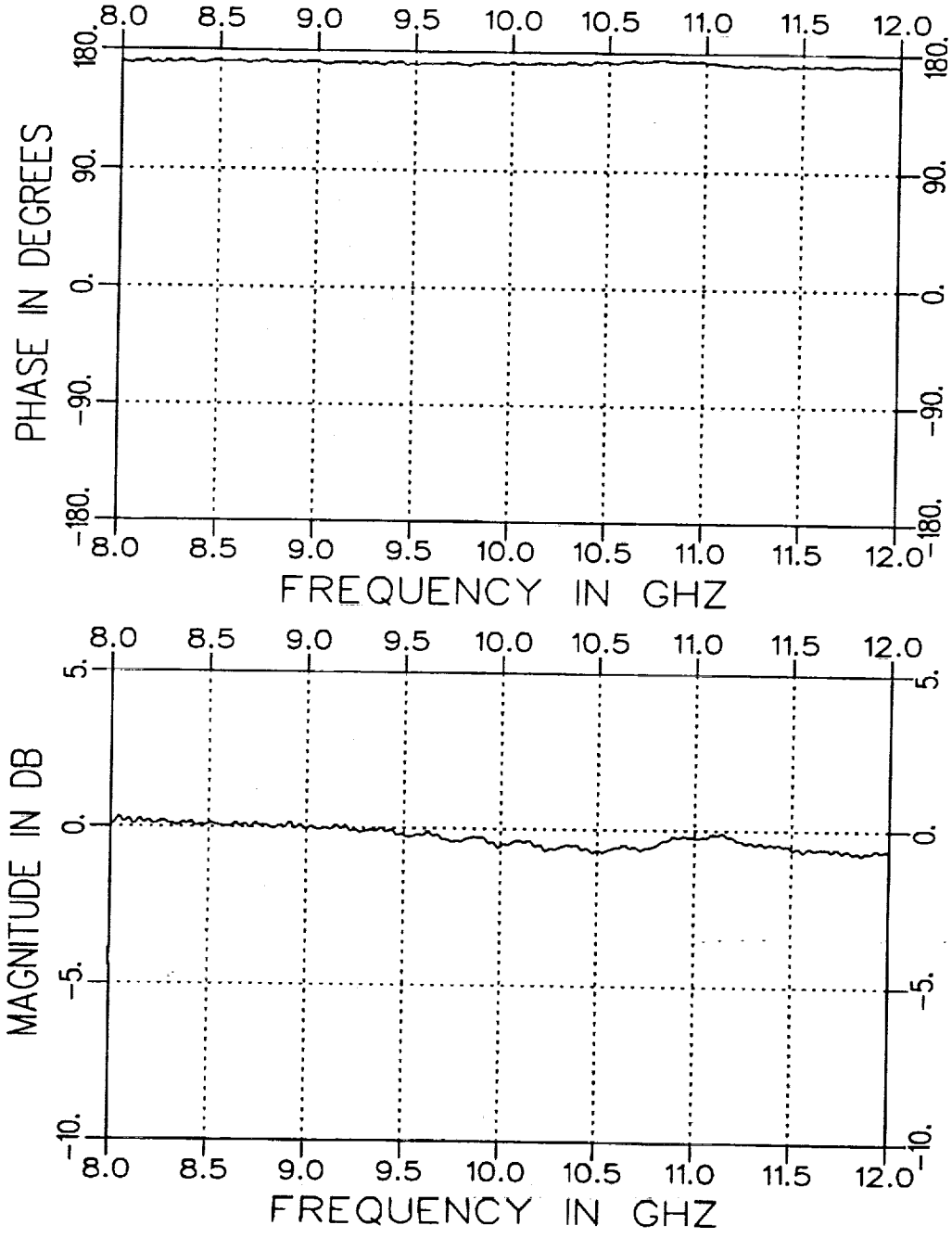

Figure 2.4: Measured reflection from a short at 400° F.

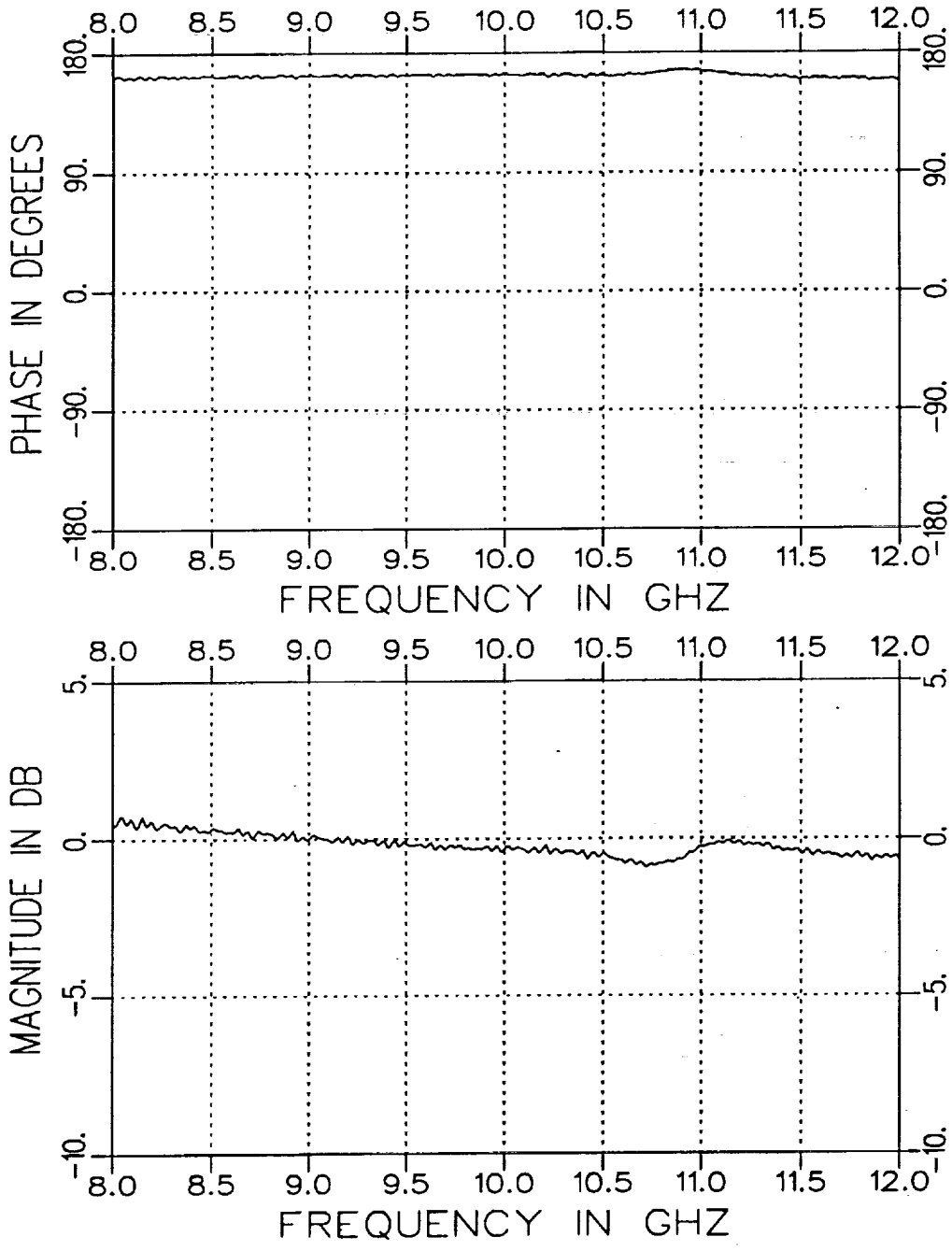

Figure 2.5: Measured reflection from a short at 500° F.

waveguide is also increasing. An analysis of the phase dependencies supports the measured results. The change in phase is a result of two components. One is dependent upon the length of the waveguide, ℓ, and the other is the width of the guide, a. Expanding the difference of the phase for two different temperatures yields,

$$\Delta\phi = \beta_{\delta a}(\ell + \delta\ell)|_{T1} - \beta_0 \ell|_{T0} \tag{2.1}$$

where $\beta_{\delta a}$ and β_0 are the propagation constants at elevated and room temperatures, respectively and δ the coefficient of linear expansion. Expanding $\beta_{\delta a}$ as a function of width yields

$$\beta_{\delta a} \simeq \beta_0 + \frac{\partial \beta_0}{\partial a}\delta a. \tag{2.2}$$

Inserting Equation (2.2) into Equation (2.1) and retaining first order terms yields

$$\Delta\phi \simeq \beta_0 \delta\ell + \frac{\partial \beta_0}{\partial a}\delta a \ell \tag{2.3}$$

where

$$\beta_0 = \frac{2\pi f}{c}\sqrt{1 - \left(\frac{c}{2af}\right)^2}. \tag{2.4}$$

Notice that the terms multiplying these two components, β_0 and $\frac{\partial \beta_0}{\partial a}$, move inversely as functions of frequency in such a way that the change in phase $\Delta\phi$ remains approximately constant ($\frac{\partial \Delta\phi}{\partial f} \simeq 0$). It was assumed that expansion occurred as a linear function of length. This assumption yields results which are in excellent agreement with measured results as shown in Figures 2.3 through 2.5.

The calibration performed at room temperature effectively removes errors due to discontinuities in the system at room temperature. When the waveguide is heated these discontinuities are no longer at the same position relative to the calibration. The calibration becomes increasingly ineffective in removing the signal error due to these discontinuities as the fixture temperature is increased. This is evident as the small ripples observed in the magnitudes of Figures 2.3 through 2.5.

Another consideration of fixture design is the mechanical resistance to physical deformation at elevated temperatures. It is felt that the wall thickness should be kept at a minimum to insure convenient uniform heating of the sample. For tested temperatures below 500° F, commercial X-band waveguides performed well as fixtures. Increasing the wall thickness would increase the amount of time and cost to heat a material sample. However, the thickness should be sufficient to locally maintain the fixture's cross section.

In conclusion, calibrating a system at room temperature and then adjusting the phase of the heated system by simply taking into consideration the change in the length of the waveguide is not a good practice. If calibrations performed at room temperature are used in measurements at elevated temperatures, the phase adjustment has to be appropriately adjusted. The observed magnitude variations are also of importance. Their correction would be impractical. As previously stated however, performing a separate calibration at each temperature achieves the best results.

Chapter 3

Parameter Extraction Methods

Three different methods of extracting the constitutive parameters from materials are considered in this chapter. All three methods consist of measuring the scattering properties (reflection and transmission) of a material sample whose electrical properties are desired. The sample(s) are placed inside a rectangular waveguide with cross sectional dimensions of the waveguide. These measurements are performed at room temperature for frequencies between 8 and 12 GHz. An HP 8510 network analyzer was used to collect the data. The data was calibrated as discussed in [5, 6]. The material sample load used in all three cases was a ceramic material with approximate constitutive parameter values of $\varepsilon_r = (8, 0)$ and $\mu_r = (1, 0)$.

In general the parameter extraction can be performed with various sample geometries as shown in Figure 3.1 [3]. The following methods used only the completely filled case.

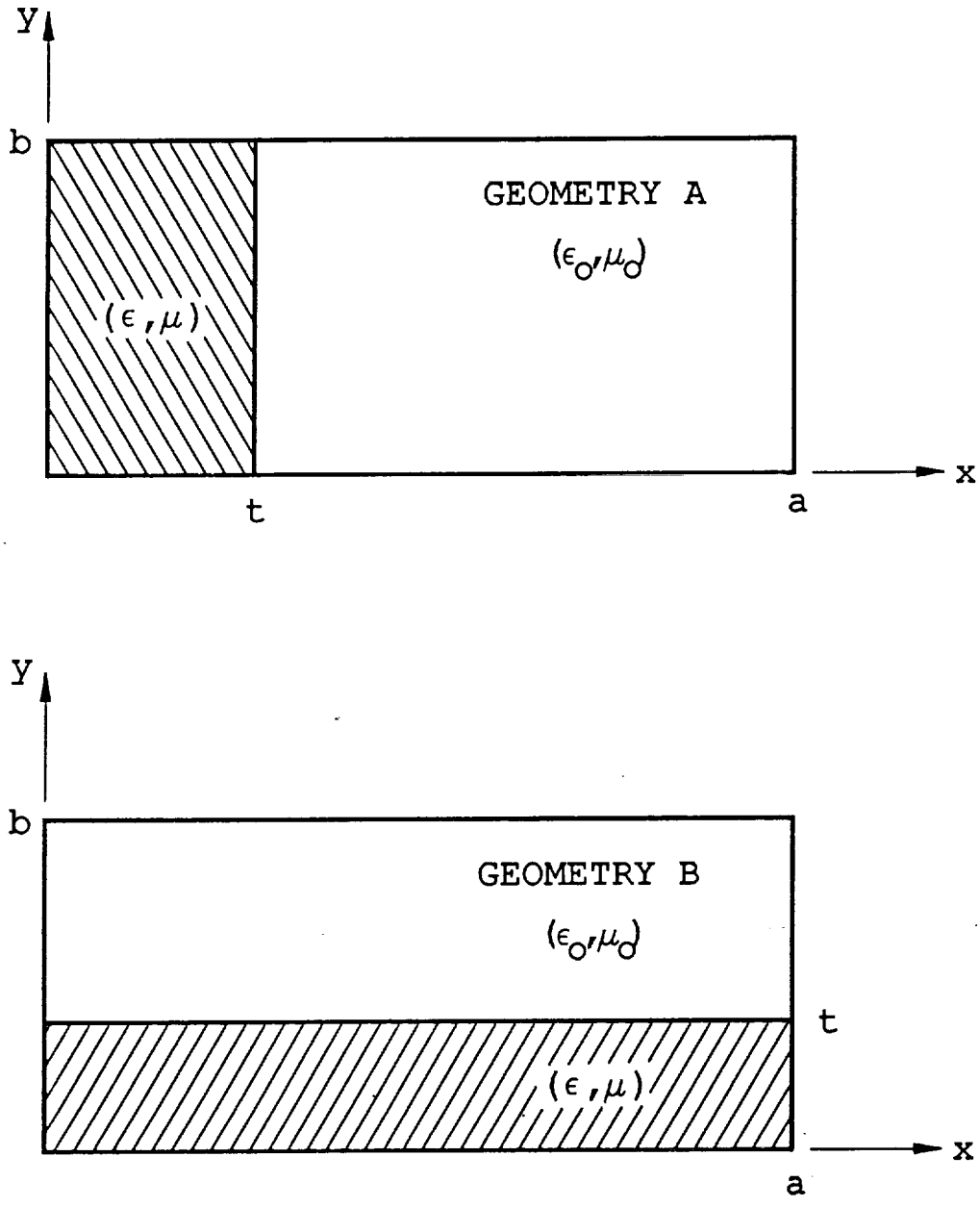

Figure 3.1: Partially-filled rectangular waveguide geometries.

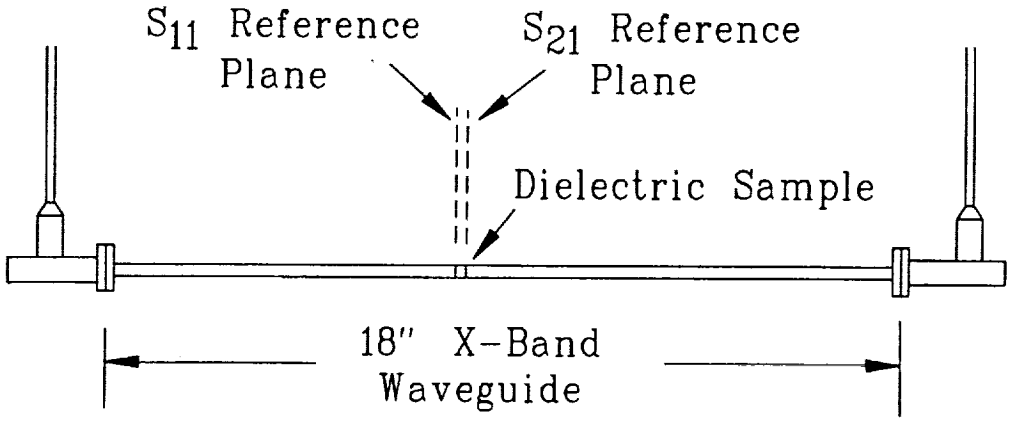

Figure 3.2: Experimental configuration for the two port extraction method.

I Two Port Method

The two port method is the traditional method of explicitly extracting the constitutive parameters from measured S_{11} (reflection) and S_{21} (transmission) parameters. The experimental configuration used in measuring the reflection and transmission coefficients is shown in Figure 3.2. The commonly used expressions to obtain the constitutive parameters are:

$$\mu_r = \frac{1+\Gamma}{1-\Gamma}\frac{\lambda_o}{\Lambda X_o} \tag{3.1}$$

and

$$\varepsilon_r = \left(\frac{1}{\Lambda^2} + \frac{1}{(2a)^2}\right)\frac{\lambda_o^2}{\mu_r} \tag{3.2}$$

where

$$\Gamma = K \pm \sqrt{K^2 - 1} \tag{3.3}$$

with

$$K = \frac{S_{11}^2 - S_{21}^2 + 1}{2S_{11}} \tag{3.4}$$

and

$$\frac{1}{\Lambda^2} = -\left[\frac{1}{2\pi d} ln \frac{1}{T}\right]^2 \tag{3.5}$$

and

$$T = \frac{S_{11} + S_{21} - \Gamma}{1 - (S_{11} + S_{21})\Gamma}. \tag{3.6}$$

Note that the sign in Equation (3.3) is chosen to insure $|\Gamma| \leq 1$, $X_o = \sqrt{1 - (\frac{\lambda_o}{2a})^2}\, d$ is the sample length, a is the waveguide width and that $ln\frac{1}{T}$ is modulo $j2\pi n$ where n is the integer of $\frac{d}{\lambda_g}$. The proper value of n can be estimated with the integer value of

$$n = \text{Int}\left[\frac{f\Phi'}{2\pi}\right] \tag{3.7}$$

where Φ' is the derivative (slope) of the phase for the transmission coefficient T with respect to frequency and f is frequency.

Notice that the thickness of the material sample, d, should be such not to form a deep null in the reflection measurement (S_{11}). Such an occurrence results in error due to a division by a small number (see Equation (3.4)).

A comparison between the extracted S_{11} and S_{21} and a calculated S_{11} and S_{21} again calculated using an $\varepsilon_r = (8, 0)$ and $\mu_r = (1, 0)$ is shown in Figures 3.3 and 3.4, respectively for a sample thickness of $d = .15$. The extracted ε_r and μ_r are shown in Figure 3.5.

Figures 3.5 and 3.6 show the real components of the relative constitutive parameters. The imaginary components were approximately equal to zero. As suggested in Figure 3.5, the extracted parameters are extremely sensitive to even slight variations in S_{11} and S_{21}. Performing frequency averaging on S_{11} and S_{21} prior to the parameter extraction improves the results as shown in Figure 3.6. As shown later, the final method considered in this chapter is much less sensitive to small variations in the measured response.

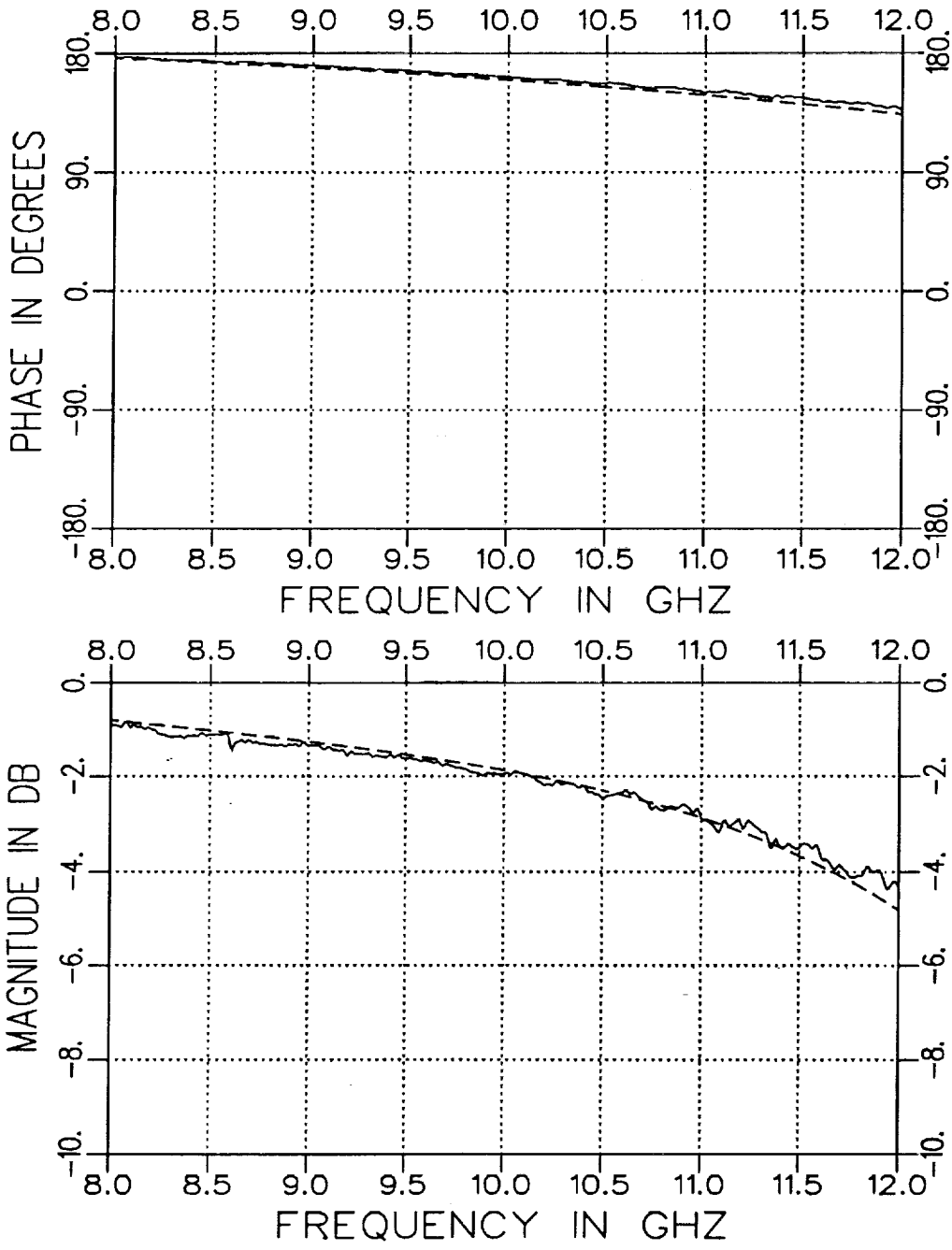

Figure 3.3: Measured (solid) and calculated (dashed) S_{11}.

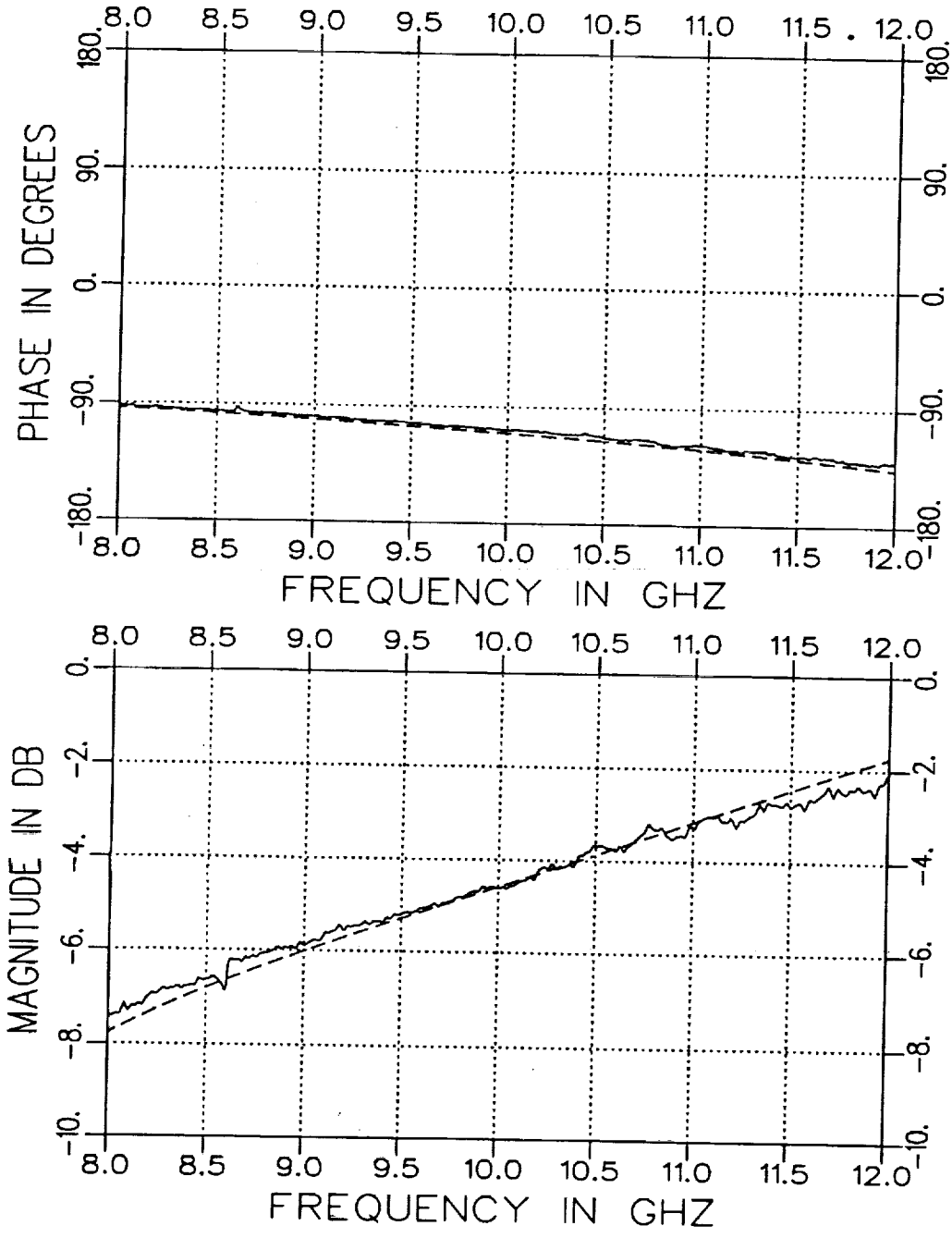

Figure 3.4: Measured (solid) and calculated (dashed) S_{21}.

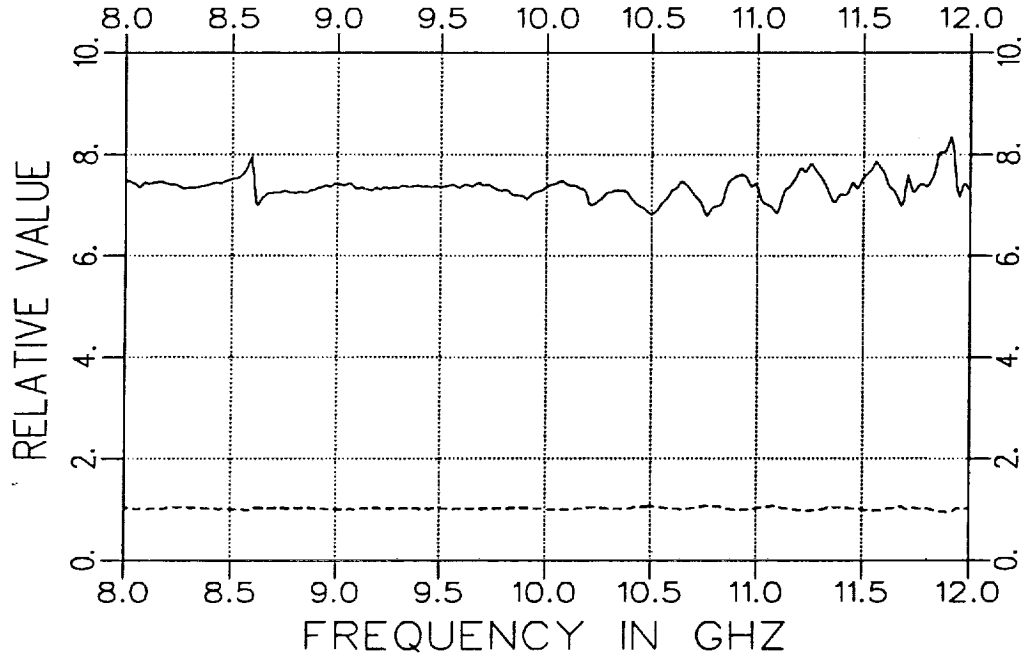

Figure 3.5: Real ϵ_r (solid) and μ_r (dashed) calculated using measured S-parameters shown in Figures 3.3 and 3.4.

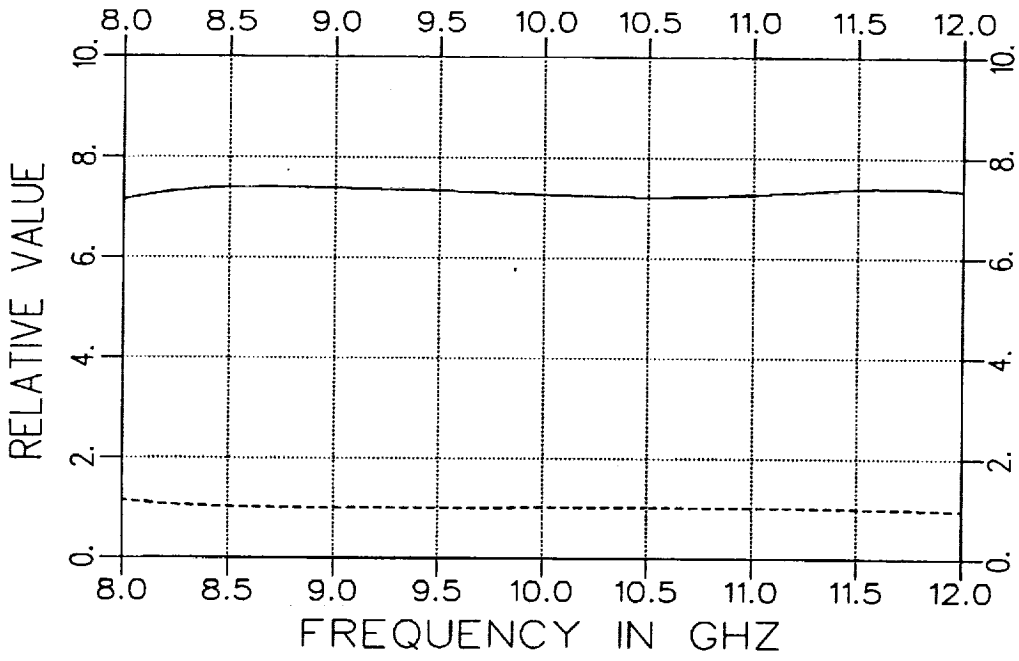

Figure 3.6: Real ϵ_r (solid) and μ_r (dashed) calculated when smoothing is applied to measured S-parameters shown in Figures 3.3 and 3.4.

II Offset Load In A Shorted Waveguide

The second method was developed to take measurements at elevated temperatures allowing the user to place a shorted waveguide containing a dielectric sample into an oven. This method has the advantage of requiring to maintain only one fixture end at room temperature. The two port method forces two fixture ends to be cooled.

This method consists of placing the sample a distance ℓ away from a short placed at the end of the waveguide. The experimental configuration is shown in Figure 3.7. The extraction of the constitutive parameters can then be accomplished from one reflection measurement using signal processing techniques to effectively recover the two port reflection and transmission measurements. Letting Γ_t represent the total reflection coefficient, the S_{11} and S_{21} scattering parameters are related as follows,

$$\Gamma_t = S_{11} - \frac{S_{21}^2 e^{-j2\beta_0 \ell}}{1 + S_{11} e^{-j2\beta_0 \ell}} \tag{3.8}$$

where β_0 is the propagation constant of the empty waveguide and ℓ is the distance from the back face of the load to the short.

Examining the response of Γ_t in the time domain Figure 3.8, a series of pulses is observed which allows the desired parameters to be obtained. Comparing the pulses in this figure to the terms Equation (3.8), the first pulse corresponds to S_{11} while the second pulse is identified as $-S_{21}^2$ once the second term of Equation (3.8) is expanded. The desired scattering parameters can then be recovered through signal processing techniques as discussed in [3].

The frequency response for the first pulse can be recovered using a moving

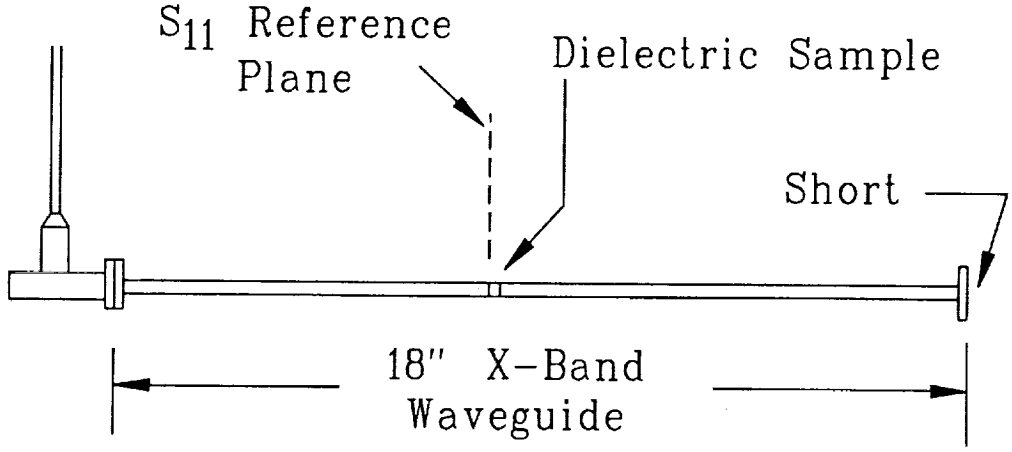

Figure 3.7: Experimental configuration for a 1-port extraction method with the sample placed a distance l from a short.

average upon the measured data Γ_t when the phase reference is centered at the front face of the sample. This is equivalent to a time domain gating approach. The moving average technique performs a weighted average around the i^{th} point using the neighborhood of n points. Increasing the value of n effectively tightens the time gating window.

The second pulse consisting of $-S_{21}^2$ can be recovered in a similar manner but first the second pulse has to be positioned at $t = 0$. This is accomplished by multiplying the measured response by a phase factor of $e^{j2\beta\ell}$. It may be necessary, depending on the thickness of the load, to add additional phase in order for the second pulse to be centered exactly at $t = 0$. This additional phase shift can be determined by simply multiplying the adjusted data by an additional phase factor until the signal is sufficiently centered. Significant distortions can occur if the pulse is not centered. After the second pulse has been isolated it is necessary to remove the additional phase factor.

Increasing the distance ℓ spreads out the pulses in the time domain. This has the effect of requiring fewer points to be averaged, and hence a broader

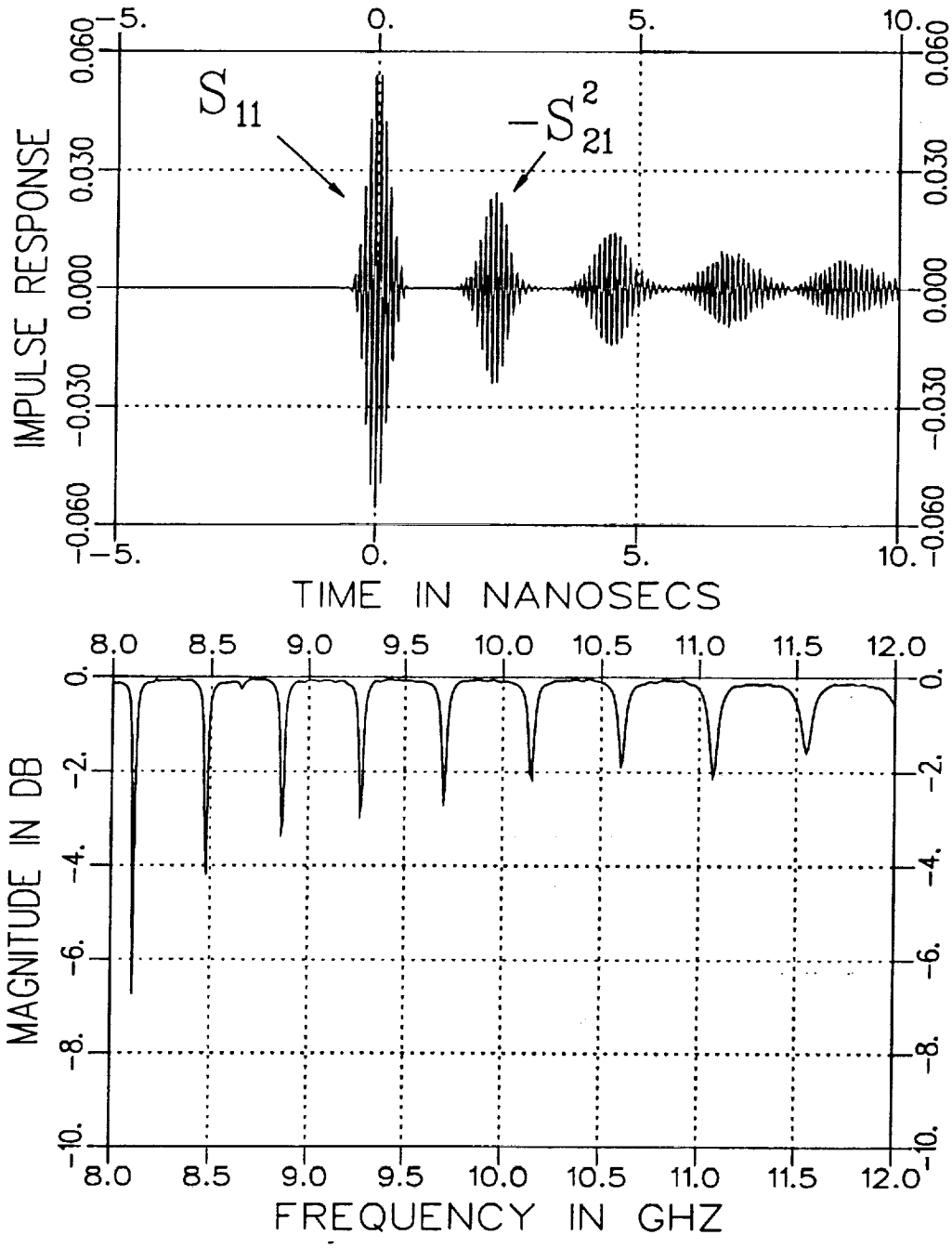

Figure 3.8: Total reflection (Γ_t) for a load placed a distance ℓ away from a short.

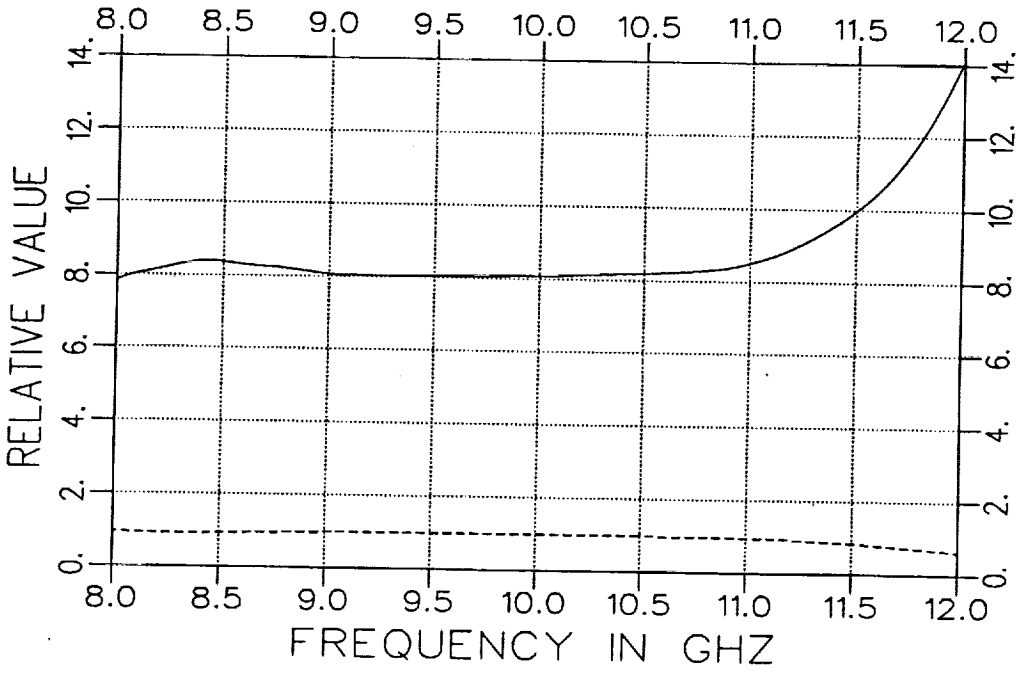

Figure 3.9: Real ϵ_r (solid) and μ_r (dashed) calculated from extracted S-parameters from data of Figure 3.8.

time domain window, when extracting the desired portion of Γ_t. Distortion in the extracted portion of the signal is reduced since the time window is more uniform about the critical portion of Γ_t. Increasing ℓ too much, however, causes the fixture to become overly frequency sensitive. It should also be noted that the required accuracy in ℓ is increased as ℓ increases.

Extracting S_{11} and S_{21} from the data of Figure 3.8, ϵ_r and μ_r can be recovered using Equations (3.1) through (3.6). The real components of relative constitutive parameters are shown in Figure 3.9. The imaginary components were again approximately equal to zero.

As indicated in Figure 3.9, the extracted constitutive parameters are reasonable in the low to mid frequency range ($8 - 11$ GHz), however the results breakdown at higher frequencies. Although this method has the desirable

quality of requiring a single reflection measurement to extract the constitutive parameters it suffers as a result of the required signal processing. The frequency averaging, although effective in removing signals about $t = 0$, also introduces distortion into the portion of the signal to be extracted. This is a result of the time window not being a perfect square filter but rather a *sinc* function about $t = 0$. In addition the uncertainty in properly positioning the S_{21} contribution at $t = 0$, for extraction constitutes an undesirable weaknesses with the method. For these reasons, a slightly different method of extracting the constitutive parameters, still using a 1-port approach, is presented in the next section.

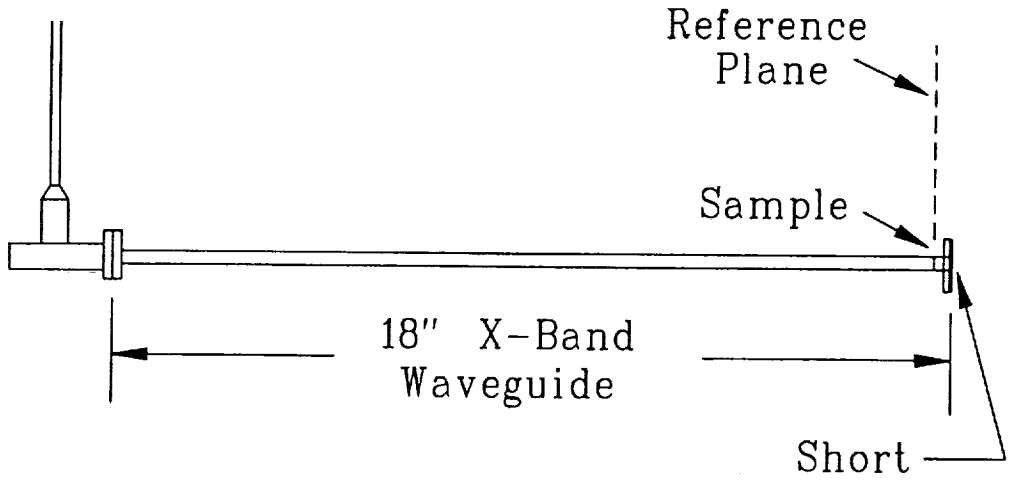

Figure 3.10: Experimental configuration for the one port method using two different sample thicknesses to extract the constitutive parameters.

III Shorted Load In A Waveguide

The final method consists of taking two reflection measurements with two different sample thicknesses d_1 and d_2. The samples in this case are to be placed against the short (i.e. $\ell = 0$) as shown in Figure 3.10. This has the benefit of not requiring a known separation distance, ℓ. An error in this distance can generate considerable error in the extracted parameter values.

The parameters can be obtained by using a Newton-Raphson iteration technique. The functionals to be driven to zero can be simply formed by the difference of the measured and calculated quantities as shown below:

$$F_1 = \Gamma_{t1}^{cal} - \Gamma_{t1}^{meas} \tag{3.9}$$

$$F_2 = \Gamma_{t2}^{cal} - \Gamma_{t2}^{meas}. \tag{3.10}$$

The search involves iterating on ϵ_r and μ_r until the following two functionals

are driven to zero. The iteration commonly takes the form of

$$\varepsilon_{r_{i+1}} = \varepsilon_{r_i} + \Delta\varepsilon_{r_i} \tag{3.11}$$

and

$$\mu_{r_{i+1}} = \mu_{r_i} + \Delta\mu_{r_i} \tag{3.12}$$

where

$$\Delta\varepsilon = \frac{F_2 \frac{\partial F_1}{\partial \mu} - F_1 \frac{\partial F_2}{\partial \mu}}{J} \tag{3.13}$$

and

$$\Delta\varepsilon = \frac{F_1 \frac{\partial F_2}{\partial \varepsilon} - F_2 \frac{\partial F_1}{\partial \varepsilon}}{J} \tag{3.14}$$

with

$$J = \begin{vmatrix} \frac{\partial F_1}{\partial \varepsilon} & \frac{\partial F_1}{\partial \mu} \\ \frac{\partial F_2}{\partial \varepsilon} & \frac{\partial F_2}{\partial \mu} \end{vmatrix}. \tag{3.15}$$

The calculated quantities can be obtained using Equation (3.8) with ℓ set to zero. The scattering parameters are calculated with the following expressions:

$$S_{11} = \frac{(1 - T^2(\varepsilon,\mu))\Gamma(\varepsilon,\mu)}{(1 - T^2(\varepsilon,\mu)\Gamma^2(\varepsilon,\mu))} \tag{3.16}$$

and

$$S_{21} = \frac{(1 - \Gamma^2(\varepsilon,\mu))T(\varepsilon,\mu)}{(1 - T^2(\varepsilon,\mu)\Gamma^2(\varepsilon,\mu))} \tag{3.17}$$

where

$$T = e^{-j\frac{\omega}{c}X_1\sqrt{\epsilon_r\mu_r}d} \tag{3.18}$$

and

$$\Gamma = \frac{\sqrt{\frac{\mu_r}{\epsilon_r}}\frac{X_o}{X_1} - 1}{\sqrt{\frac{\mu_r}{\epsilon_r}}\frac{X_o}{X_1} + 1} \tag{3.19}$$

where $X_o = \sqrt{1 - (\frac{\lambda_o}{2a})^2}$ and $X_1 = \sqrt{1 - (\frac{\lambda_o}{2a\sqrt{\epsilon_r\mu_r}})^2}$ with λ_o being the free space wavelength, c the speed of light and a is the width of the rectangular guide.

The measured S_{11}^{thin} and S_{11}^{thick} are shown in Figures 3.11 and 3.12, respectively. The real components of the relative constitutive parameters ϵ_r and μ_r are shown in Figure 3.13. It is interesting to note that although the quality of the measured response is comparable to that used in the two port example, the extracted parameters are much smoother. This method appears to be less sensitive to the small variations that exist in actual measurements. The explanation for this stability appears to be due to the need of only one calibration reference unlike the two port method where two calibration references are needed.

The next chapter employs this method to extract the constitutive parameters when the waveguide/sample is heated.

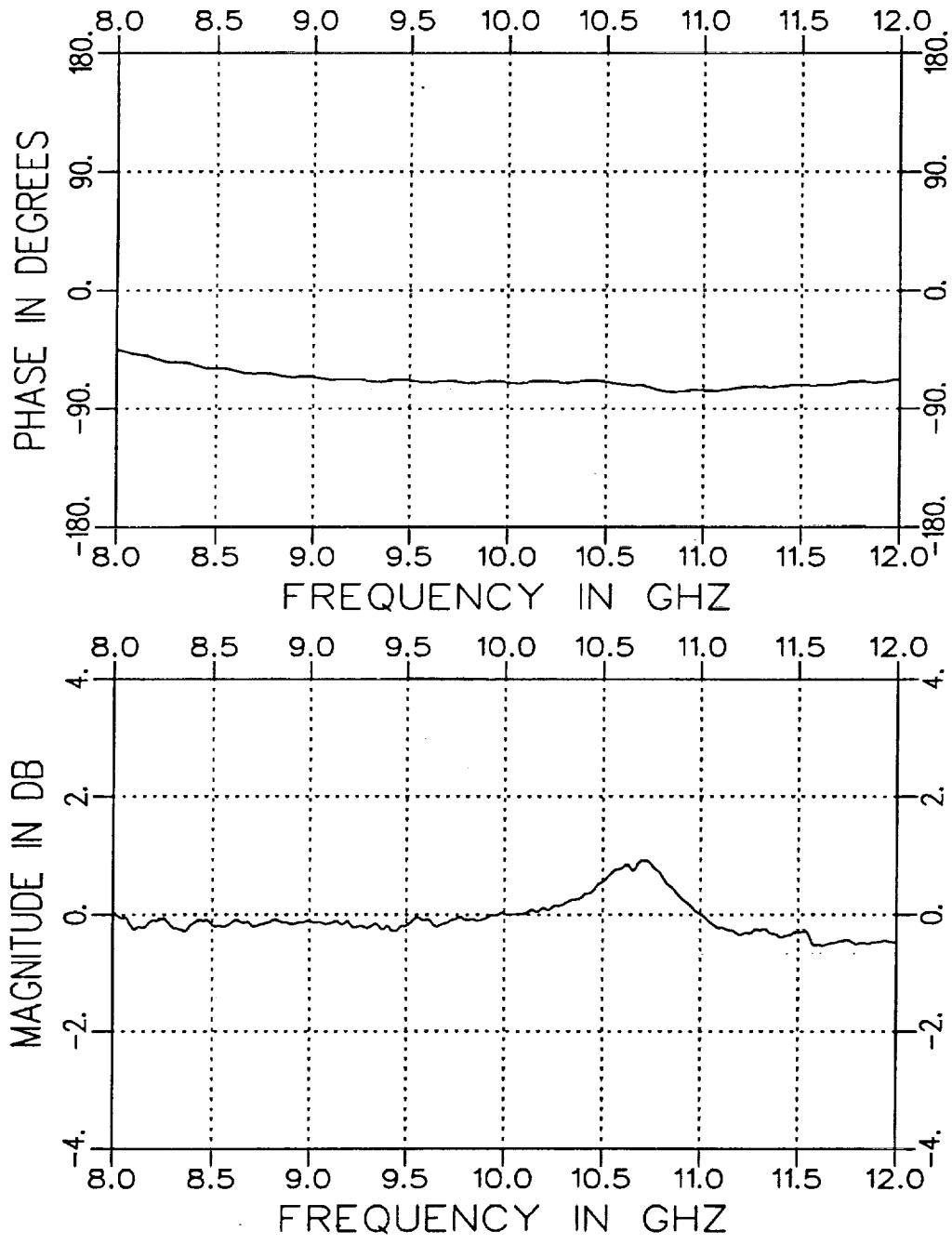

Figure 3.11: Measured S_{11}^{thin} for a load thickness $d = .15$ inches.

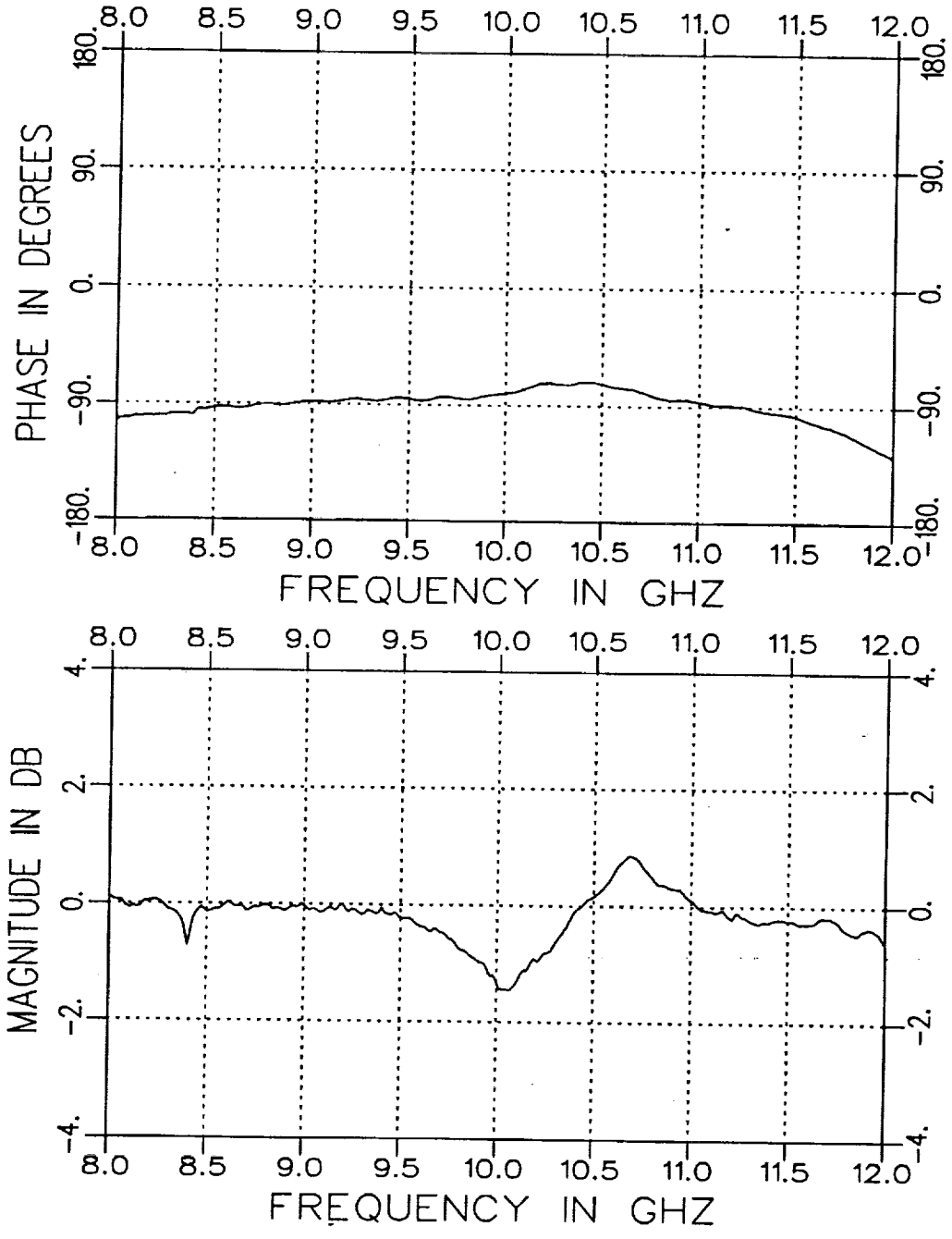

Figure 3.12: Measured S_{11}^{thick} for a load thickness $d = .254$ inches.

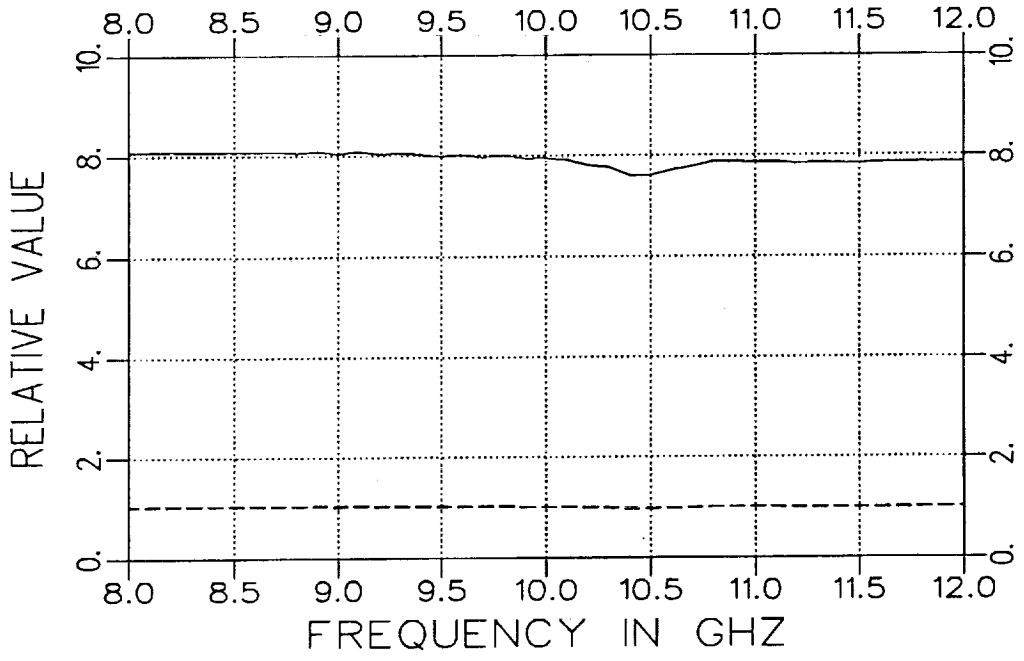

Figure 3.13: Real ϵ_r (solid) and μ_r (dashed) extracted using the 1-port, with 2 different sample thicknesses method.

Chapter 4

Extraction Performance at Elevated Temperatures

The best method for extracting material parameters appears to be to make two reflection measurements with a short placed at the rear face of the sample. The most accurate constitutive parameters can be acquired if the sample can fill the cross section of the guide for the desired temperature. Significant gaps resulting from thermal expansion can be accounted for as indicated in [3]. For small gaps the approximate formulas in [4] may be of value.

Figure 4.1 illustrates the experimental setup used to extract the desired S_{11} measurements. Two different fixtures were used in acquiring elevated temperature measurements. The simplest fixture consisted of commercially available copper X-band waveguide. This fixture worked well for the moderate elevated temperatures considered here ($< 500°$ F). A second waveguide was fabricated from 316 stainless steel to withstand oxidation and fixture deformation considerations experienced at higher temperatures. The advantage of the first fixture occurs with its thinner wall thickness in comparison to the thicker wall thickness of the second fixture. Using a fixture with thinner walls allows fast heating times which is very desirable for very elevated temperatures. The need for thicker walls arises from the requirement to maintain

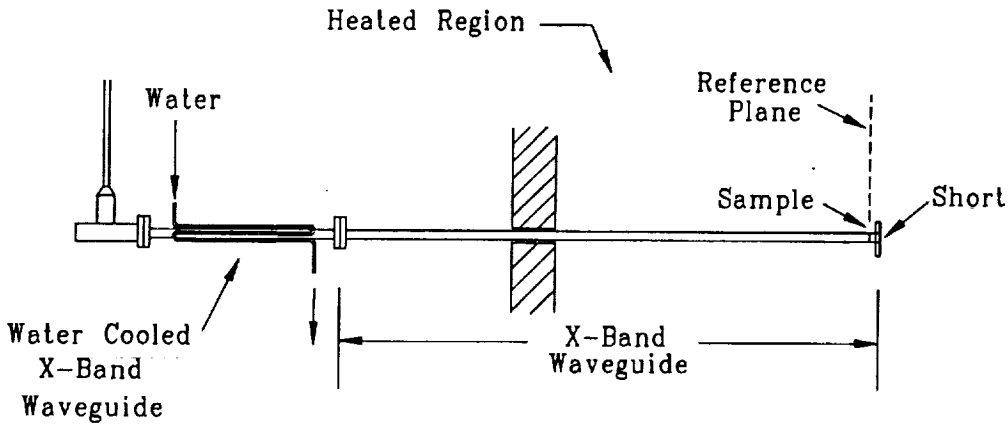

Figure 4.1: Experimental configuration for the heated 1-port method using two different sample thicknesses to extract the constitutive parameters.

an uniform and straight interior fixture cross section. Figures 4.2 and 4.3 illustrates the stainless steel fixture used.

Figures 4.4 through 4.6 represent extracted values for the relative constitutive parameters for the ceramic load used in the previous chapter at several temperatures. These measurements were made using the thin walled copper alloy fixture. Although the material sample used did not undergo any profound changes as a function of temperature, the results clearly indicate the effectiveness of this method in extracting the parameters when the sample is heated.

The calibration used for these measurements involved a unique calibration set for each temperature. The collection of measured data involved in this chapter consisted first of performing the necessary reflection measurements to determine the calibration constants at each temperature. Next, the reflection measurements for each material sample are performed at each temperature.

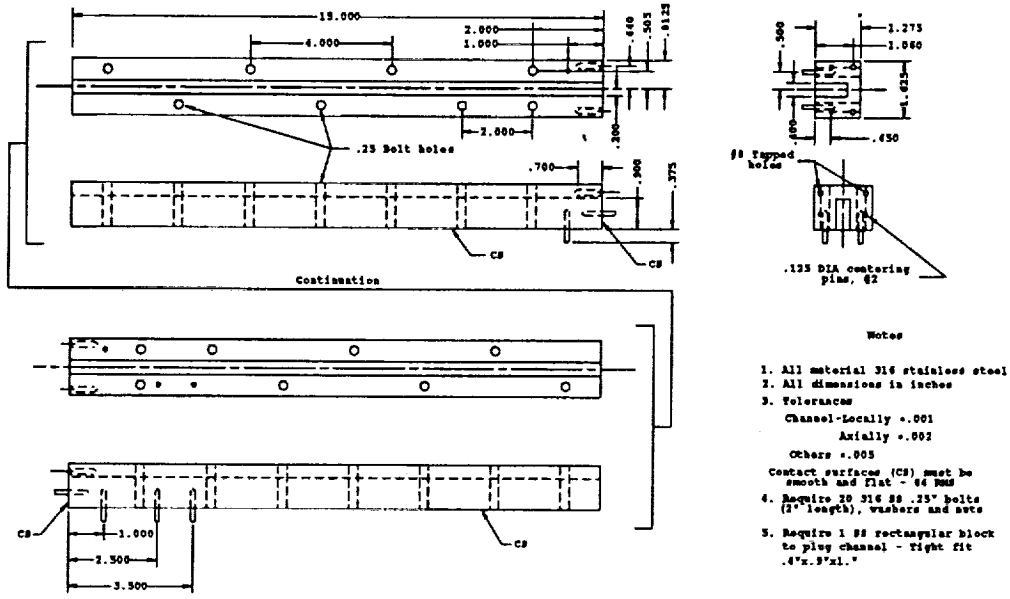

Figure 4.2: Mechanical drawing for stainless steel, X-band waveguide fixture.

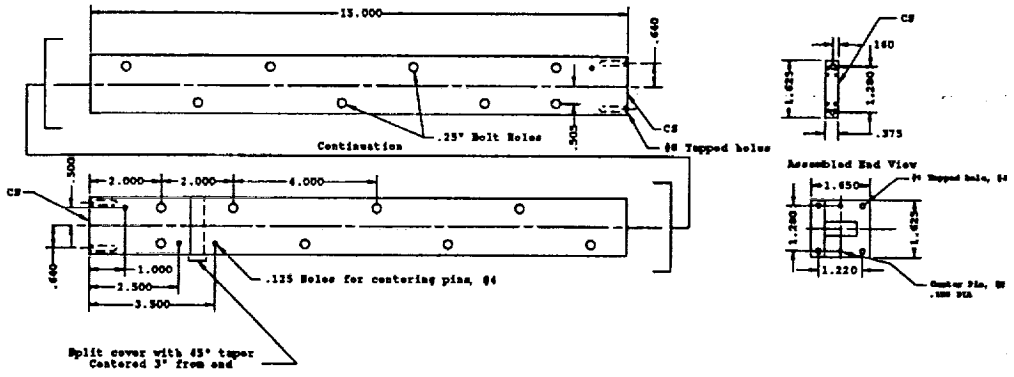

Figure 4.3: Mechanical drawing for stainless steel, X-band waveguide fixture.

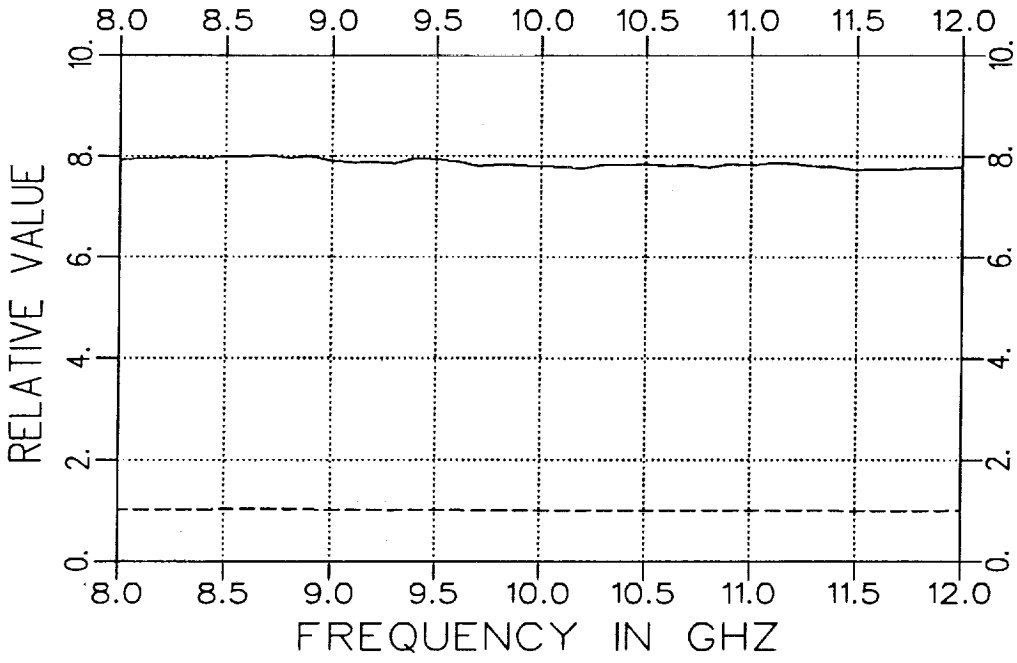

Figure 4.4: Real components of extracted ε_r (solid) and μ_r (dashed) for a ceramic load at 300° F.

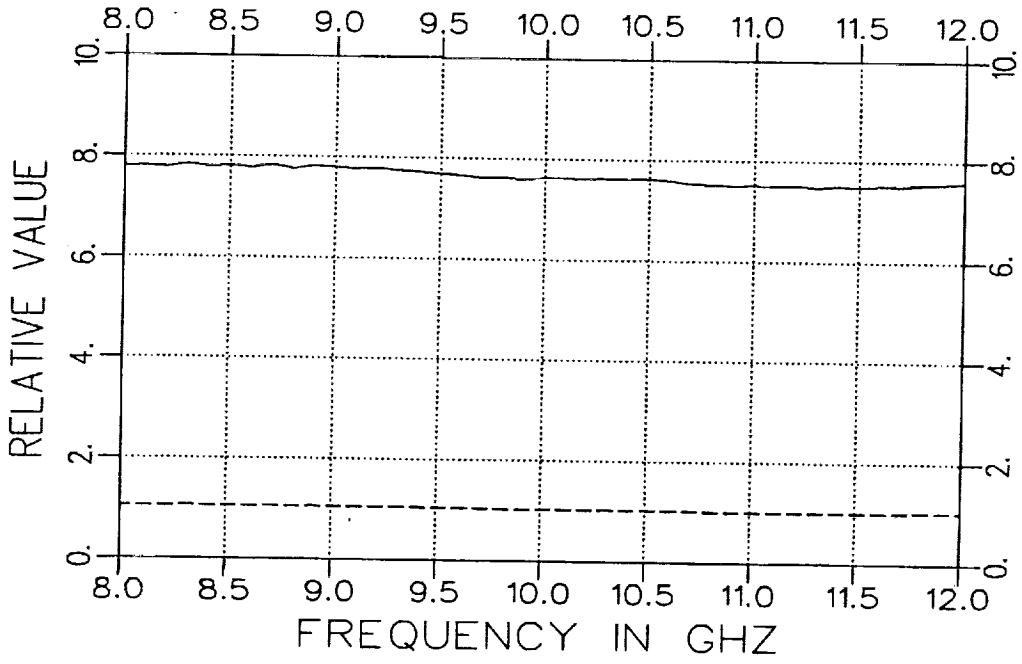

Figure 4.5: Real components of extracted ϵ_r (solid) and μ_r (dashed) for a ceramic load at 400° F.

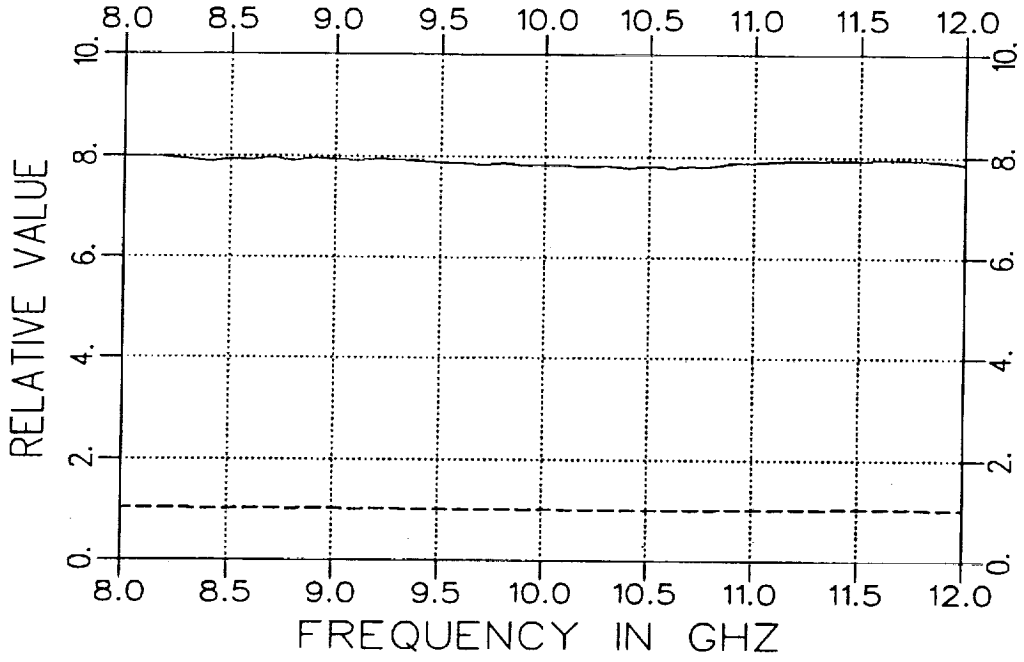

Figure 4.6: Real components of extracted ϵ_r (solid) and μ_r (dashed) for a ceramic load at 500° F.

Chapter 5

Conclusions

Three different methods of extracting constitutive parameters from a sample placed in a waveguide fixture were examined. The three methods consisted of a 2-port approach, a 1-port approach with the sample placed a distance ℓ from a short, and a 1-port approach using two different sample thicknesses placed against a short. The final method was found to yield the best results. This is believed to be a result of requiring only one type of calibration procedure (reflection). Potentially, errors might result when an inconsistency may exist between independent calibrated reflection and transmission measurements.

The 1-port approach, using two different sample thicknesses, was then used to extract the constitutive parameters when the sample end of the fixture was heated in an electric oven. The results of these measurements demonstrated the effectiveness of this method in extracting constitutive parameters when the sample is heated.

Finally, it should be emphasized that, due to the sensitivity in the extraction process, it is strongly recommended that calibrations be performed at each temperature when performing the parameter extractions at elevated temperatures.

Bibliography

[1] R.F. Harringtion, Time Harmonic Electromagnetic Fields, McGraw-Hill Book Company, New York, 1961.

[2] M.N. Afsar, J.R. Birch and R.N. Clarke, " The Measurement of the Properties of Material," Proceedings of the IEEE, Vol. 74, No. 1, January 1986.

[3] A. Park and A Dominek, "Constitutive Parameter De-embedding Using Inhomogeneously-Filled Rectangular Waveguides with Longitudinal Section Modes," Report No. 721837-2, The ElectroScience Laboratory, The Ohio State University, October 1990; Prepared under Grant Number NSG3-1000, NASA Lewis Research Center.

[4] Handbook of Microwave Measurements, Edited by M. Wind and H. Rapaport, Polytechnic Institute of Brooklyn, Vol. 1, Section X, Appendix I, p. 29, 1955.

[5] J. Munk and A Dominek, "Calibration of Automatic Network Analyzers," Report No. 723224-1, The ElectroScience Laboratory, The Ohio State University, September 1990; Prepared under Grant Number NSG3-1108, NASA Lewis Research Center.

[6] H. Sequeira and R. Jakhete, "New Calibration Simplifies MMIC Wafer Probing," Microwaves & RF, July 1988.